# Influence of alkali metal superoxides on structure, electronic, and optical properties of $Be_{12}O_{12}$ nanocage: Density functional theory study

Ali Raoof Toosi, Hamid Reza Shamlouei†, and Asghar Mohammadi Hesari

*Lorestan University, Chemistry Department, Khorram Abad, Iran*

(Received 10 February 2016; revised manuscript received 12 May 2016; published online 19 July 2016)

The effect of alkali metal superoxides $M_3O$ ($M$ = Li, Na, K) on the electronic and optical properties of a $Be_{12}O_{12}$ nanocage was studied by density functional theory (DFT) and time-dependent density functional theory (TD-DFT). The energy gaps ($E_g$) of all configurations were calculated. Generally, the adsorption of alkali metal superoxides on the $Be_{12}O_{12}$ nanocage causes a decrease of $E_g$. Electric dipole moment $\mu$, polarizability $\alpha$, and static first hyperpolarizability $\beta$ were calculated and it was shown that the adsorption of alkali metal superoxides on $Be_{12}O_{12}$ increases its polarizability. It was found that the absorption of $M_3O$ on $Be_{12}O_{12}$ nanocluster improves its nonlinear optical properties. The highest first hyperpolarizability ($\beta \approx 214000$ a.u.) is obtained in the $K_3O$–$Be_{12}O_{12}$ nanocluster. The TD-DFT calculations were performed to investigate the origin of the first hyperpolarizabilities and it was shown that a higher first hyperpolarizability belongs to the structure that has a lower transition energy.

**Keywords:** $Be_{12}O_{12}$, alkali metal superoxides, hyperpolarizability, DFT calculation

**PACS:** 42.70.Nq, 42.70.Mp **DOI:** 10.1088/1674-1056/25/9/094220

## 1. Introduction

Materials with large nonlinear optical (NLO) properties are very useful for optical interconnections, optical switching, and signal processing.[1,2] The accurate theoretical determination of hyperpolarizability can make significant contributions to explore new nonlinear optical materials with potential applications in advanced technologies.[3]

Cages with fullerene-like structures can be utilized in new industrial applications such electronic devices, imaging materials, magnetic recording and environmental processes.[4–10] These cages with another substituent lead to the emergence of some physical properties such as a different energy gap and genesis of semiconducting properties.[11–15] Nanocages with the $M_{12}X_{12}$ formula are most stable energetically among different types of $(MX)_n$ structures.[16–22] Moreover theoretical studies demonstrated that the $M_{12}X_{12}$ cluster built from square and hexagonal rings is more stable than that built from pentagons and hexagons.[22–24] Previously some studies were done to improve the NLO properties of nanocages. For instance, lithium, sodium, and potassium were employed to increase the NLO properties of $Mg_{12}O_{12}$ and $B_{12}O_{12}$ nanocages,[25] and similarly transition metal atoms were used to improve the $Mg_{12}O_{12}$ nanocage.[26] Wu *et al.* used the alkali superoxide ($M_3O$) to improve the NLO properties of materials and designed novel alkalides with high NLO properties.[27]

In the present work, we report a theoretical study on the interaction of alkali metal superoxides with the $Be_{12}O_{12}$ nanocage. Structure, energetic, electronic, and optical properties of the compounds are studied using density functional theory.

## 2. Computational details

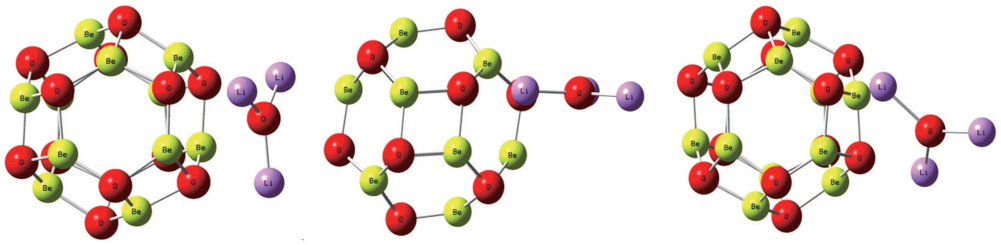
The optimized structures of ground state of $Be_{12}O_{12}$ nanocage, $M_3O$ ($M$ = Li, Na, K), and complex of $Be_{12}O_{12}$ with $M_3O$ ($M_3O$@$Be_{12}O_{12}$) were calculated using density functional theory at the B3LYP/6-311+G(d) level.[28–32]

To find the optimized structures for $M_3O$ ($M$ = Li, Na, K) adsorbed on the surface of $Be_{12}O_{12}$, several different initial configurations were used for optimization: (i) three metal atoms horizontally attached on three oxygen atoms in the hexagonal ring of $Be_{12}O_{12}$ (3$M$-H-3O h ring), (ii) two metal atoms vertically attached on two oxygen atoms in the hexagonal ring of $Be_{12}O_{12}$ ($M$-V-2O-h ring), (iii) two metal atoms vertically attached on two oxygen atoms in the square ring of $Be_{12}O_{12}$ (2$M$-V-2O-s ring). These configurations are illustrated in Fig. 1.

All calculations were performed using the Gaussian 09W.[33] The electronic density of states (DOS) for all structures was calculated using the GaussSum program.[34] The spin-unrestricted approach was applied to describe the geometry optimization, electronic structure, and NLO properties of the $M_3O$–$Be_{12}O_{12}$ nanocluster and the functional Coulomb-attenuated hybrid exchange–correlation functional (CAM-B3LYP)[35] was used to predict the large molecular system. This functional also provided good quality results for the electronic excitation energies.[36–39]

†Corresponding author. E-mail: shamlouei.ha@lu.ac.ir

© 2016 Chinese Physical Society and IOP Publishing Ltd 



(a) 3*M*-H-3O h ring (b) 2*M*-V-2O h ring (c) 2*M*-V-2O S ring

**Fig. 1.** (color online) Different scenarios of $M_3O$ on $Be_{12}O_{12}$: (a) 3*M*-H-3O h ring, three *M* metals sit horizontally on a three O atoms hexagonal ring, (b) 2*M*-V-2O-h ring, two *M* metals sit vertically on a two O atoms hexagonal ring, (c) 2*M*-V-2O-s ring, two *M* metals sit vertically on a two O atoms square ring.

The electronic properties of the cluster including the frontier molecular orbitals, which correspond to the highest occupied molecular orbital (HOMO) and the lowest unoccupied molecular orbital (LUMO), ionization potential ($I$), electron affinity ($A$), chemical potential ($\mu$), global hardness ($\eta$), softness (S), global electrophilicity ($\omega$), index electronegativity ($\chi$) and the maximum amount of electronic charge index ($\Delta N_{\max}$) were calculated. All the electronic properties can be obtained through the HOMO–LUMO orbitals.[40–47] The calculated HOMO-LUMO energy gap $E_g$, chemical hardness $\eta$, chemical potential $\mu$, electrophilicity index $\omega$, and maximum amount of electronic charge index $\Delta N_{\max}$ are in atomic units.

The simplest polarizability $\alpha$ characterizes the ability of an electric field to distort the electronic distribution of a molecule related to the linear optical properties. Higher order polarizabilities (hyperpolarizabilities $\beta$, $\gamma$, etc.) describe the nonlinear response of atoms and molecules related to a wide range of phenomena in nonlinear optics.[48] The energy of an uncharged liner molecule in a weak, homogenous electric field can be written as

$$E = E^0\mu_i F_i - 1/2\alpha_{ij}F_iF_j - 1/6\beta_{ijk}F_iF_jF_k - 1/24V_{ijkl}F_iF_jF_kF_l + \cdots,$$

where $E^0$ is the energy of the unperturbed molecule, $F_i$ is the field at the origin $\mu_i$ , and $\alpha_{ij}$, $\beta_{ijk}$, and $V_{ijkl}$ are the components of the dipole moment, i.e., the polarizability, the first and the second order hyperpolarizability, respectively.

Using the two-level model,[49–51] the relation between the hyperpolarizibility and other time dependent properties are obtained by the following relation:

$$\beta_0 \propto \frac{f_0\Delta\mu}{\Delta E^3},$$

where $\Delta E$, $f$, and $\Delta\mu$ are the transition energy, the oscillator strength, and the difference in the dipole moments between the ground state and the crucial excited state respectively. In this model, $\beta$ is inversely proportional to $\Delta E^3$, so $\Delta E$ is the decisive factor in the first hyperpolarizability.[52–54]

Because of the dependence of the first hyperpolarizability on the ground state and the excited state properties, the time-dependent density functional theory (TD-DFT) calculations at the CAM-B3LYP/6-31+G(d) level were performed to obtain the excitation energy and the differences of the dipole moments between the ground state and the excited state as well as the oscillator strength $f_0$.

## 3. Results and discussion

### 3.1. Geometrical structure

The optimized structures and geometrical parameters of the $Be_{12}O_{12}$ nanocage are depicted in Fig. 2. As seen in Fig. 2, the $Be_{12}O_{12}$ nanocage consists of six square and eight hexagonal rings. Two different bonds exist within this nanocage: one is shared between two hexagons (hh) and the other is between a square ring and a hexagon (hs). The bond lengths ($l$) of hh-bonds and hs-bonds in $Be_{12}O_{12}$ nanoclusters are 1.520 Å and 1.577 Å, respectively, which is in accordance with Ref. [25]. The density of states plots for the $Be_{12}O_{12}$ nanocage are shown in Fig. 2. The energies of HOMO ($\varepsilon_{\text{HOMO}}$) and LUMO ($\varepsilon_{\text{LUMO}}$) as well as the energy gap ($E_g$) calculated from the DOS spectrum are −8.64 eV, −1.04 eV, and 7.60 eV, respectively, which confirms the semiconductor character of the nanocage. After optimization of the $Be_{12}O_{12}$ nanocage, the $M_3O$ superoxides were placed in different sites of it (Fig. 1), and then their structures were optimized. The optimized structures of the $M_3O$–$Be_{12}O_{12}$ nanoclusters are depicted in Figs. 3–5.

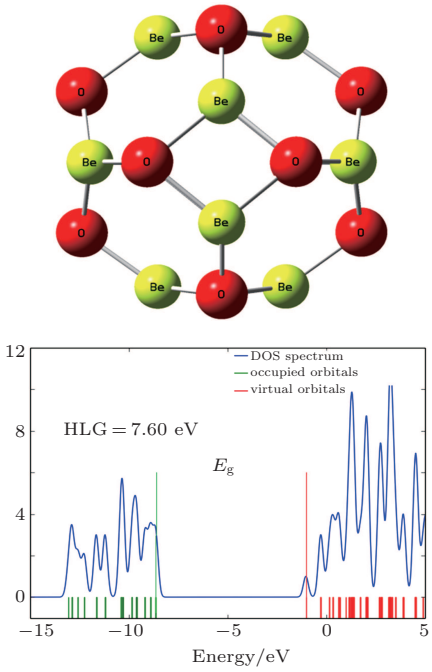



**Fig. 2.** (color online) The optimized geometry of the pristine $Be_{12}O_{12}$ nanocluster.

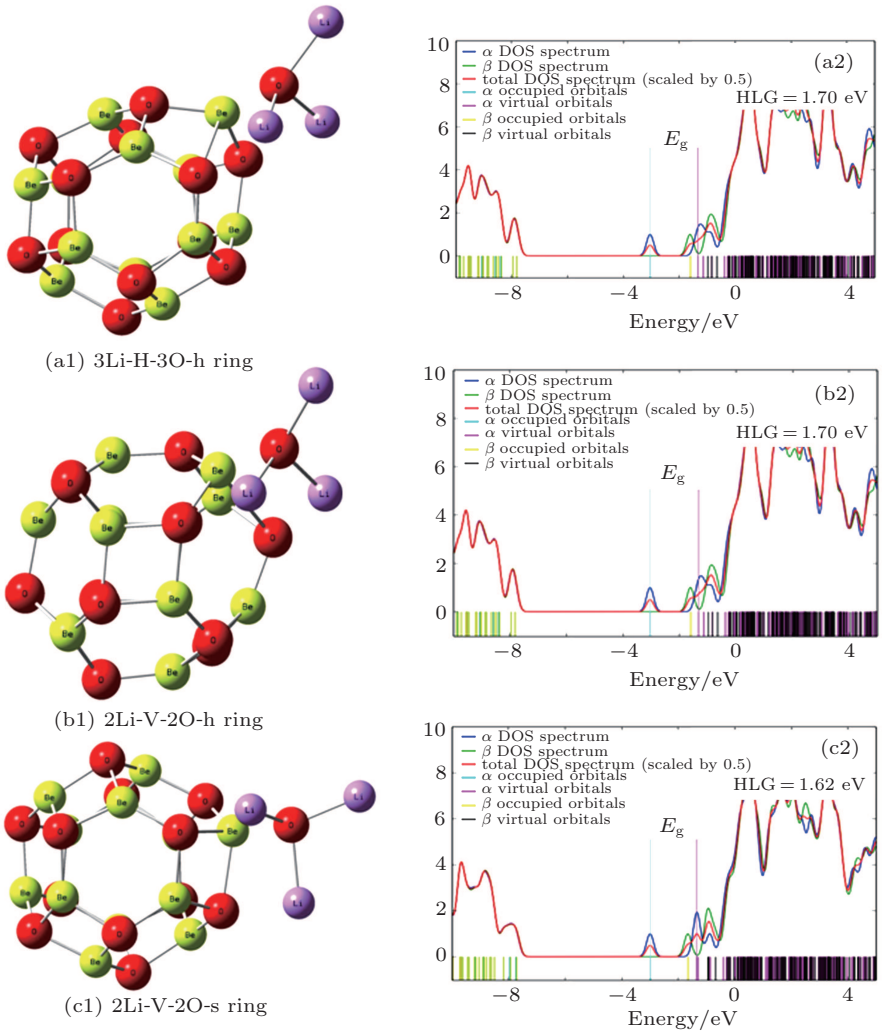
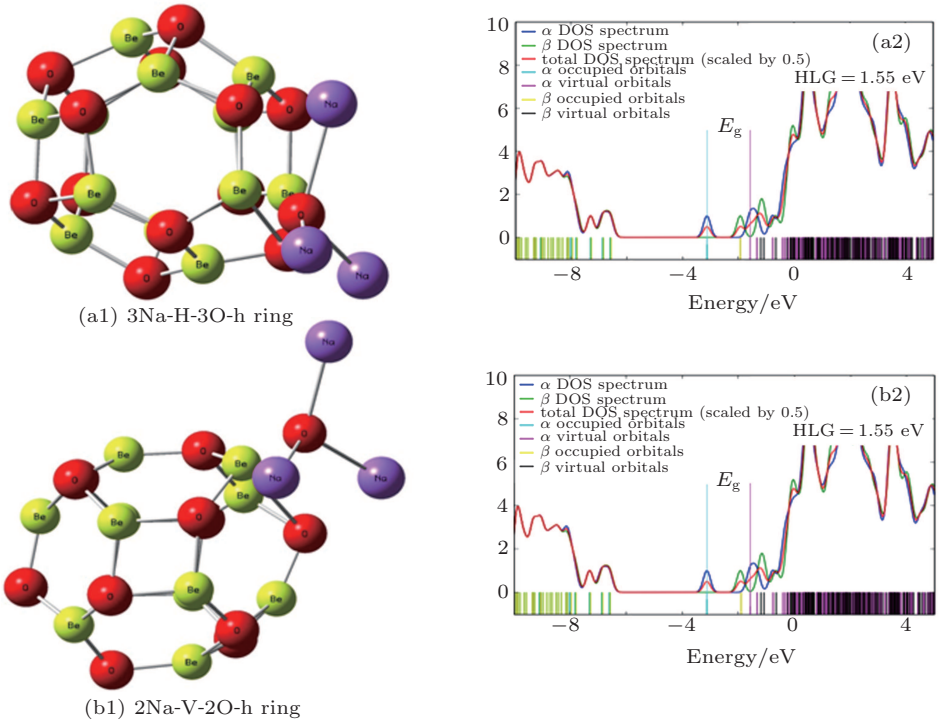



**Fig. 3.** (color online) The structures and the total density of states of the $Be_{12}O_{12}$ nanocluster beside $Li_3O$ super alkali metal after optimization at the B3LYP/6-311+g(d) level: (a) 3Li-H-3O h ring, (b) 2Li-V-2O-h ring, (c) 2Li-V-2O-s ring.



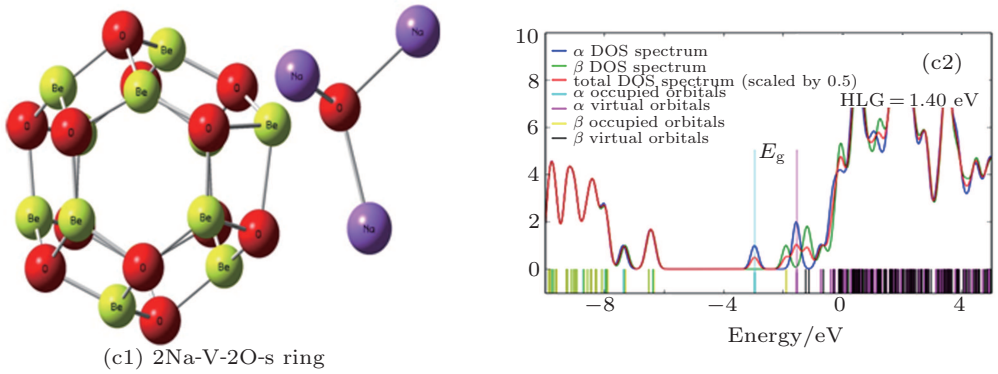



**Fig. 4.** (color online) The structures and the total density of states of the $Be_{12}O_{12}$ nanocluster beside $Na_3O$ super alkali metal after optimization at the B3LYP/6-311+g(d) level: (a) 3Na-H-3O h ring, (b) 2Na-V-2O-h ring, (c) 2Na-V-2O-s ring.

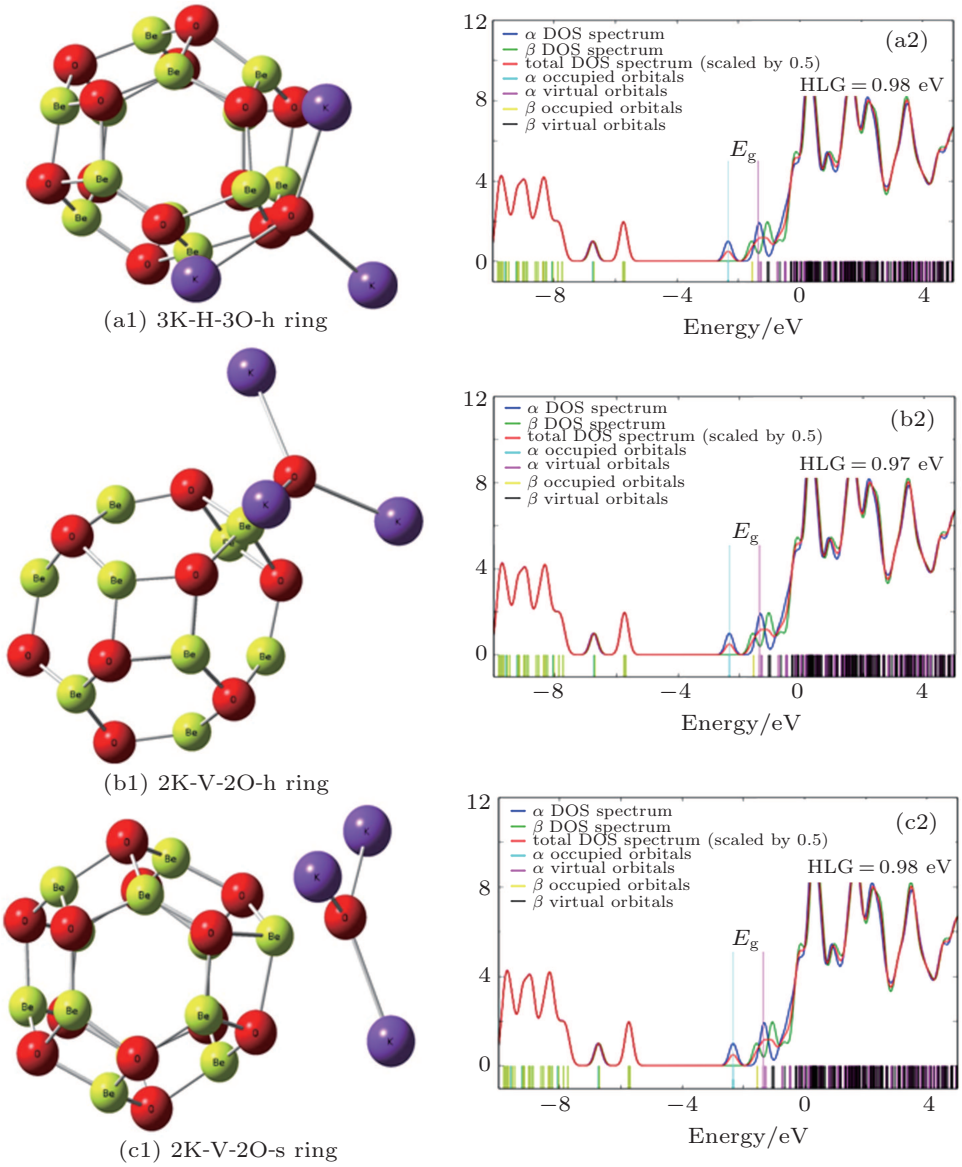



**Fig. 5.** (color online) The structures and the total density of states of the $Be_{12}O_{12}$ nanocluster beside $K_3O$ super alkali metal after optimization at the B3LYP/6-311+g(d) level: (a) 3K-H-3O h ring, (b) 2K-V-2O-h ring, (c) 2K-V-2O-s ring.

The bond lengths of Be–O located between two hexagonal rings (hh) and a hexagonal ring and a square ring for the $M_3O$–$Be_{12}O_{12}$ nanocage are listed in Table 1. As seen in Table 1, the existence of $M_3O$ on the surface of the $Be_{12}O_{12}$ nanocage drastically affects its structure and highly deforms it. According to Table 1, the larger effect is seen in the $Na_3O$ case and the smaller effect is observed in the $K_3O$ case, especially for the 2D structure. Both interaction distances between $M$ of the superoxide and O of the $Be_{12}O_{12}$ nanocage was studied and the results are gathered in Table 2.

**Table 1.** The bond lengths of Be–O in hh and hs rings for all optimized structures of $M_3O$–$Be_{12}O_{12}$.

| Fig. | Configuration | Be–O(hh)/Å | Be–O(hs)/Å |
|---|---|---|---|
| 2 | pristine | 1.52 | 1.58 |
| 3(a) | 3Li-H-3O-h ring | 1.64 | 2.50 |
| 3(b) | 2Li-V-2O-h ring | 1.64 | 2.49 |
| 3(c) | 2Li-V-2O-s ring | 1.56 | 1.86 |
| 4(a) | 3Na-H-3O-h ring | 1.65 | 2.64 |
| 4(b) | 2Na-V-2O-h ring | 1.65 | 2.64 |
| 4(c) | 2Na-V-2O-s ring | 1.60 | 1.89 |
| 5(a) | 3K-H-3O-h ring | 1.68 | 1.82 |
| 5(b) | 2K-V-2O-h ring | 1.56 | 1.82 |
| 5(c) | 2K-V-2O-s ring | 1.68 | 1.82 |

**Table 2.** Interaction distance (in units of Å) between M or O of $M_3O$ and Be or O of $Be_{12}O_{12}$.

| $Li_3O$–$Be_{12}O_{12}$ | | $Na_3O$–$Be_{12}O_{12}$ | | $K_3O$–$Be_{12}O_{12}$ | |
|---|---|---|---|---|---|
| Li3-O6 | 1.810 | Na2-O8 | 2.179 | O8-K2 | 2.715 |
| Li4-O10 | 1.925 | Na3-O6 | 2.327 | O6-K3 | 2.742 |
| O1-Be5 | 1.510 | Be7-O1 | 1.489 | Be7-O1 | 1.502 |

As seen in Table 1, the interaction distances between Li atoms in the $Li_3O$–$Be_{12}O_{12}$ case are lower than those in the $Na_3O$–$Be_{12}O_{12}$ and $K_3O$–$Be_{12}O_{12}$ cases, which may be the result of the smaller atomic diameter of lithium. For all configurations, the binding energies which are related to the feasibility of forming $M_3O@Be_{12}O_{12}$ were calculated and reported in Table 3. Among these systems, $K_3O@Be_{12}O_{12}$ has the highest binding energy and is more stable than the others.

**Table 3.** The binding energy of the system for all considered configurations.

| Fig. | Configuration | $E_b$/kcal·mol$^{-1}$ |
|---|---|---|
| 3(a) | 3Li-H-3O-h ring | –19.29 |
| 3(b) | 2Li-V-2O-h ring | –19.29 |
| 3(c) | 2Li-V-2O-s ring | –17.11 |
| 4(a) | 3Na-H-3O-h ring | –26.93 |
| 4(b) | 2Na-V-2O-h ring | –26.93 |
| 4(c) | 2Na-V-2O-s ring | –24.58 |
| 5(a) | 3K-H-3O-h ring | –27.65 |
| 5(b) | 2K-V-2O-h ring | –27.65 |
| 5(c) | 2K-V-2O-s ring | –27.65 |

## 4. Electronic properties

The HOMO and LUMO orbitals and the calculated energy gap for all considered conformations are gathered in Table 4. As seen in Table 4 (and mentioned previously), the obtained HOMO and LUMO energies and consequently $E_g$ for pristine $Be_{12}O_{12}$ are $-8.64$ eV, $-1.04$ eV, and 7.6 eV, respectively. It is shown that the HOMO and LUMO energies are lowered by the $M_3O$ presence. However, a larger decrease takes place on the HOMO energy, so $E_g$ reduces for all $M_3O$–$Be_{12}O_{12}$ nanocages. Moreover, the highest reduction in $E_g$ occurs in the case of $K_3O$–$Be_{12}O_{12}$ ($-89.87\%$). The $M_3O$ molecules have high densities of electrons, their excess electrons are injected to the clusters via interaction and a new HOMO level with higher energy locating between the original HOMO and LUMO of the pristine cluster is formed, this may explain the narrowing of the $E_g$.

**Table 4.** Electric properties of the pristine form and $M_3O$ adsorbed $Be_{12}O_{12}$ nanocages.

| Fig. | Configuration | HOMO | LUMO | $E_g$ | $\mu$ | $\omega$ | $I$ | $A$ | $n$ | $\eta$ | $\chi$ | $\Delta N_{max}$ | $\Delta E_g$ |
|---|---|---|---|---|---|---|---|---|---|---|---|---|---|
| 2 | pristine | –8.64 | –1.04 | 7.60 | –4.84 | 3.08 | 8.64 | 1.04 | 0.26 | 3.80 | 4.84 | 1.27 | 0.00 |
| 3(a) | 3Li-H-3O-h ring | –3.03 | –1.60 | 1.43 | –2.32 | 3.75 | 3.03 | 1.60 | 1.40 | 0.72 | 2.32 | 3.24 | –81.18 |
| 3(b) | 2Li-V-2O-h ring | –3.03 | –1.60 | 1.43 | –2.32 | 3.75 | 3.03 | 1.60 | 1.40 | 0.72 | 2.32 | 3.24 | –81.18 |
| 3(c) | 2Li-V-2O-s ring | –2.98 | –1.65 | 1.33 | –2.32 | 4.03 | 2.98 | 1.65 | 1.50 | 0.67 | 2.32 | 3.48 | –82.50 |
| 4(a) | 3Na-H-3O-h ring | –3.11 | –1.91 | 1.20 | –2.51 | 5.25 | 3.11 | 1.91 | 1.67 | 0.60 | 2.51 | 4.18 | –84.21 |
| 4(b) | 2Na-V-2O-h ring | –3.11 | –1.91 | 1.20 | -2.51 | 5.25 | 3.11 | 1.91 | 1.67 | 0.60 | 2.51 | 4.18 | –84.21 |
| 4(c) | 2Na-V-2O-s ring | –2.95 | –1.89 | 1.06 | –2.42 | 5.52 | 2.95 | 1.89 | 1.89 | 0.53 | 2.42 | 4.57 | –86.05 |
| 5(a) | 3K-H-3O-h ring | –2.32 | –1.55 | 0.77 | –1.94 | 4.86 | 2.32 | 1.55 | 2.60 | 0.39 | 1.94 | 5.03 | –89.87 |
| 5(b) | 2K-V-2O-h ring | –2.32 | –1.55 | 0.77 | –1.94 | 4.86 | 2.32 | 1.55 | 2.60 | 0.39 | 1.94 | 5.03 | –89.87 |
| 5(c) | 2K-V-2O-s ring | –2.32 | –1.55 | 0.77 | –1.94 | 4.86 | 2.32 | 1.55 | 2.60 | 0.39 | 1.94 | 5.03 | –89.87 |

The other quantum chemical quantities such as chemical potential $\mu$, global electrophilicity $\omega$, ionization potential $I$, electron affinity $A$, softness $S$, global hardness $\eta$, index electronegativity $\chi$, and maximum amount of electronic charge index $\Delta N_{max}$, which are related to $E_g$, were calculated for all optimized conformations and given in Table 4.

### 4.1. Optical properties

The electric dipole moment $\mu$, polarizability $\alpha$, and first order static hyperpolarizability $\beta$ of pristine $Be_{12}O_{12}$ and $M_3O$–$Be_{12}O_{12}$ were calculated using DFT theory at the CAM-B3LYP/6-31+G (d,p) level. The dipole moments of the mentioned structures are presented in Table 5. The dipole moment obtained for pristine $Be_{12}O_{12}$ is 0 Debye and the surprising order of the dipole moment increasing is as follows: $Li_3O$–$Be_{12}O_{12}$ <$K_3O$–$Be_{12}O_{12}$ <$Na_3O$–$Be_{12}O_{12}$.

**Table 5.** Calculated dipole moments for all configurations. All components and $\mu_{tot}$ are in units of Debye.

| Fig. | Configuration | $\mu_x$ | $\mu_y$ | $\mu_z$ | $\mu_{tot}$ |
|---|---|---|---|---|---|
| 2 | pristine | 0.000 | 0.000 | 0.000 | 0.000 |
| 3(a) | 3Li-H-3O-h ring | 0.016 | 0.441 | –0.203 | 0.486 |
| 3(b) | 2Li-V-2O-h ring | –0.019 | 0.448 | -0.210 | 0.495 |
| 3(c) | 2Li-V-2O-s ring | 0.196 | 0.003 | –0.440 | 0.481 |
| 4(a) | 3Na-H-3O-h ring | –1.732 | 0.499 | –0.711 | 1.938 |
| 4(b) | 2Na-V-2O-h ring | 1.733 | 0.506 | –0.713 | 1.941 |
| 4(c) | 2Na-V-2O-s ring | –1.396 | 0.001 | –1.046 | 1.744 |
| 5(a) | 3K-H-3O-h ring | 1.486 | 0.434 | –0.008 | 1.548 |
| 5(b) | 2K-V-2O-h ring | 1.487 | 0.466 | –0.005 | 1.558 |
| 5(c) | 2K-V-2O-s ring | –1.486 | 0.426 | –0.007 | 1.546 |

**Table 6.** Polarizability, polarizability variation, and first hyperpolarizability of all structures. The values are in units of a.u.

| Fig. | $\alpha_0$ | $\Delta\alpha$ | $\beta^0$ |
|---|---|---|---|
| 2 | 127.5 | 0 | 0.000 |
| 3(a) | 373.6 | 153.7 | 23592.4 |
| 3(b) | 374.1 | 153.5 | 23762.5 |
| 3(c) | 433.7 | 220.7 | 34439.1 |
| 4(a) | 458.3 | 208.1 | 37527.4 |
| 4(b) | 458.7 | 208.8 | 37638.8 |
| 4(c) | 591.5 | 341.4 | 87280.4 |
| 5(a) | 1388.9 | 1076.0 | 200422.1 |
| 5(b) | 1387.1 | 1075.0 | 214101.2 |
| 5(c) | 1389.1 | 1076.1 | 195730.1 |

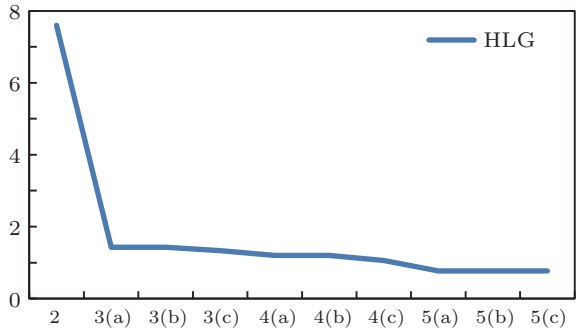



**Fig. 6.** (color online) The energy gaps $E_g$ of $Be_{12}O_{12}$ nanoclusters for all configuraions.

The polarizability $\alpha$ and the first hyperpolarizability for all structures were calculated and reported in Table 6. The minimum polarizability is observed in the interaction with $Li_3O$, and the highest polarizability is observed in the interaction with $K_3O$. Additionally, the polarizability improvement which can be seen as the result of $K_3O$ adsorption on the $Be_{12}O_{12}$ nanocage is considerable in comparison to others. Similarly, it is observed that the first hyperpolarizability of the nanocage is considerably enhanced by the $M_3O$ adsorption. The $K_3O$ adsorbed on $Be_{12}O_{12}$ leads to the highest first hyperpolarizability improvement. The dipole moment, polarizability, and first hyperpolarizability are plotted simultaneously to show their trends in Fig. 7.

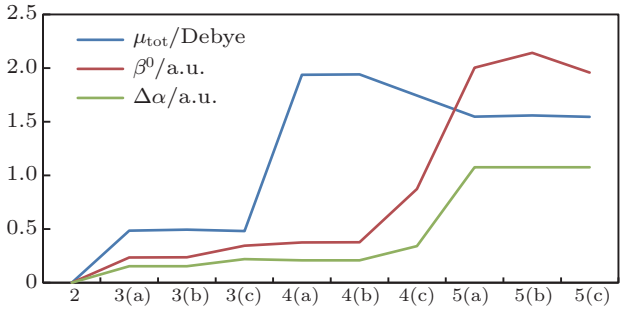



**Fig. 7.** (color online) Relationships of dipole moment, polarizability, and first order hyperpolarizability.

## 4.2. TD-DFT

Time-dependent density functional theory calculations at the CAM-B3LYP/6-31+G(d) level were used to obtain the transition excited state properties such as excitation energies $E$ and oscillator strengths $f$. The major electric transition CT and transition moment of all configurations are listed in Table 7.

**Table 7.** TD-CAM-B3LYP/6-31+g(d) calculated results of transition energy $\Delta E_{gn}$, transition moment $\mu_{gn}$, oscillator strength $f_{ng}$, and the major electric transitions obtained for all conformations.

| Fig. | Configuration | $\Delta E$/eV | $\beta/10^{-5}$ a.u. | $\Delta\mu_{g-e}$/a.u. | $f$/a.u. | $S^2$ | CT[a] |
|---|---|---|---|---|---|---|---|
| 2 | pristine | 7.5305 | 0.0000 | 0.1642 | 0.0050 | 0.00 | H→L |
| 3(a) | 3Li-H-3O-h ring | 1.2140 | 0.2359 | 2.1937 | 0.2135 | 0.75 | H→L |
| 3(b) | 2Li-V-2O-h ring | 1.2120 | 0.2376 | 2.1856 | 0.2133 | 0.75 | H→L |
| 3(c) | 2Li-V-2O-s ring | 1.0923 | 0.3444 | 2.2203 | 0.1953 | 0.75 | H→L |
| 4(a) | 3Na-H-3O-h ring | 1.1256 | 0.3753 | 1.1077 | 0.2558 | 0.75 | H→L |
| 4(b) | 2Na-V-2O-h ring | 1.1246 | 0.3764 | 1.1070 | 0.2560 | 0.75 | H→L |
| 4(c) | 2Na-V-2O-s ring | 0.9688 | 0.8728 | 1.3248 | 0.2235 | 0.75 | H→L |
| 5(a) | 3K-H-3O-h ring | 0.5874 | 2.0042 | 2.7085 | 0.2607 | 0.75 | H→L |
| 5(b) | 2K-V-2O-h ring | 0.5866 | 2.1410 | 2.6960 | 0.2601 | 0.75 | H→L |
| 5(c) | 2K-V-2O-s ring | 0.5876 | 1.9573 | 2.7111 | 0.2608 | 0.75 | H→L |

[a]H and L refer to the HOMO and LUMO, respectively.

The modifications of hyperpolarizibility $\beta$ for all structures are compared to energy changes $\Delta E_{gn}$ in Fig. 8. In Fig. 8, it is clearly seen that the excitation energy inversely relates to the hyperpolarizibility. A small change of the transition energy leads to a drastic change in hyperpolarizability (with inverse of 3 powers). Configuration 3(a) has the largest transition energy $\Delta E_{gn}$ which corresponds to the smallest hyperpolarizability $\beta$. On the other hand, the minimum $\Delta E_{gn}$ and the maximum first hyperpolarizability belong to $K_3O$–$Be_{12}O_{12}$, which corresponds to the results obtained previously.

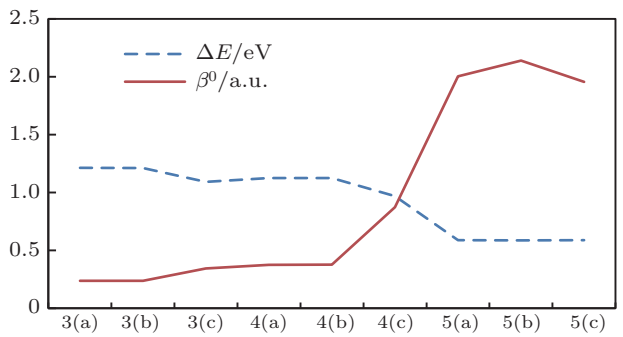



**Fig. 8.** (color online) The first hyperpolarizibility and excitation energy for different configurations.

## 5. Conclusion

We performed DFT study of the effect of $M_3O$ on the structure, electric and optical properties of $Be_{12}O_{12}$ nanocluster to suggest a way to improve its NLO properties. It was found that the adsorption of super alkali metals on $Be_{12}O_{12}$ leads to decreased $E_g$ and increased polarizability. The hyperpolarizibility is drastically affected by the presence of super alkali metals. The $K_3O$–$Be_{12}O_{12}$ has the highest change in hyperpolarizibility by about 200000 a.u. The relation between the transition energy $\Delta E_{gn}$ and the first hyperpolarizability $\beta$ was explored by TD-DFT calculations.

## References


[1] Geskin V M, Lambert C and Breda J L 2003 *Am. Chem. Soc.* **125** 15651
[2] Sajan D, Joe H, Jayakumar V S and Zaleski J 2006 *Mol. Struct.* **785** 43
[3] Bredas J L, Adant C, Tackx P, Persoons A and Pierce B M 1994 *Chem. Rev.* **94** 243
[4] Sorokin P B, Fedorov A S and Chernozatonskii L A 2006 *Phys. Solid State.* **48** 398
[5] Baumeier B, Krüger P and Pollmann J 2007 *Phys. Rev. B* **76** 085407
[6] Zhao M, Xia Y, Li F, Zhang R Q and Lee S T 2005 *Phys. Rev. B* **71** 085312
[7] Ma L C, Zhao H S and Yan W J 2013 *Magn. Magn. Mater.* **330** 174
[8] Fabiański R, Firlej L, Zahab A and Kuchta B 2002 *Solid State Sci.* **4** 1009
[9] Jalbout A F 2009 *Comp. Mater. Sci.* **44** 1065
[10] Lee J H, Lee B S, Au F T K, Zhang J and Zeng Y 2012 *Comp. Mater. Sci.* **56** 131
[11] Paine R T and Narula C K 1990 *Chem. Rev.* **90** 73
[12] Wu H S, Zhang F Q, Xu X H, Zhang C J and Jiao H 2003 *Phys. Chem. A* **107** 204
[13] Zhu H Y, Schmalz T G and Klein D J 1997 *Int. Quantum Chem.* **63** 393
[14] Goldberg D, Bando Y, Stephan O and Kurashima K 1998 *Appl. Phys. Lett.* **73** 2441
[15] Wang Q, Sun Q, Jena P and Kawazoe Y 2009 *ACS Nano.* **3** 621
[16] Xu S H, Zhang M Y, Zhao Y Y, Chen B G, Zhang J and Sun C C 2006 *Chem. Phys. Lett.* **423** 212
[17] Jain A, Kumar V and Kawazoe Y 2006 *Comp. Mater. Sci.* **36** 258
[18] Hong L, Wang H, Cheng J, Tang L and Zhao J 2012 *Comp. Theor. Chem.* **980** 62
[19] Beheshtian J, Bagheri Z, Kamfiroozi M and Ahmadi A 2012 *Mol. Model.* **18** 2653
[20] Kakemam J and Peyghan A A 2013 *Comp. Mater. Sci.* **79** 352
[21] Shakerzadeh E 2014 *Inorg. Organomet. Polym.* **24** 694
[22] Jensen F and Toftlund H 1993 *Chem. Phys. Lett.* **201** 89
[23] Strout D L 2000 *Phys. Chem. A* **104** 3364
[24] Strout D L 2001 *Phys. Chem. A* **105** 261
[25] Shakerzdeh E, Tahmasebi E and Shamlouei H R 2015 *Synthetic Metals* **204** 17
[26] Shamlouei H R, Nouri A, Mohammadi A and Tehrani A D 2016 *Physica E* **77** 48
[27] Sun W M, Fan L T, Li Y, Liu J.Y, Wu D and Li Z R 2014 *Inorg. Chem.* **53** 6170
[28] Becke A D 1993 *J. Chem. Phys.* **98** 5648
[29] Lee C, Yang W and Parr R G 1988 *Phys. Rev. B* **37** 785
[30] Krishnan R, Binkley J S, Seeger R and Pople J A 1980 *J. Chem. Phys.* **72** 650
[31] Mclean A D and Chandler G S 1980 *J. Chem. Phys.* **72** 5639
[32] Blaudeau J P, McGrath M P, Curtiss L A and Radom L 1997 *J. Chem. Phys.* **107** 5016
[33] Frisch M J and *et al.* 2009 *Gaussian 09* Revision A.1 (Gaussian Inc: Wallingford CT)
[34] O'Boyle N M, Tenderholt A L and Langner K M 2008 *Comput. Chem.* **29** 839
[35] Yanai T, Tew D P and Handy N C 2004 *Chem. Phys. Lett.* **393** 51
[36] Alparone A 2013 *Chem. Phys. Lett.* **563** 88
[37] Yanai T, Hariison R J and Handy N C 2005 *Mol. Phys.* **103** 413
[38] Peach M J G, Helgaker T, Saiek P, Keal T W, Lutnas O B, Tozer D J and Handy N C 2006 *Phys. Chem. Chem. Phys.* **8** 558
[39] Kobayashi R and Amos R D 2006 *Chem. Phys. Lett.* **420** 106
[40] Pearson R G 1990 *Coord. Chem. Rev.* **100** 403
[41] Lewis D F V, Ioannides C and Parke D V 1994 *Xenobiotica* **24** 401
[42] Zhou Z and Parr R G 1990 *Am. Chem. Soc.* **112** 5720
[43] Franke R 1984 *Theoretical Drug Design Methods* (London: Elsevier Science)
[44] Fleming I 1976 *Molecular Orbitals and Organic Chemical Reactions* (London: John Wiley & Sons)
[45] Fukui K 1975 *Theory of Orientation and Stereo Selection* (New York: Springer-Verlag)
[46] Fukui K 1982 *Angenwandte. Chem.* **21** 801
[47] Beheshtian J, Peyghan A A and Bagheri Z 2012 *Appl surf. Sci.* **258** 8980
[48] Kleinman D A 1962 *Phys. Rev.* **126** 1977
[49] Oudar J L and Chemla D S 1977 *J. Chem. Phys.* **66** 2664
[50] Oudar J L 1977 *J. Chem. Phys.* **67** 446
[51] Kanis D R, Ratern M A and Marks T J 1994 *Chem. Rev.* **94** 195
[52] Ayan D and Swapan K P 2006 *Chem. Soc. Rev.* **35** 1305
[53] Parr R G, Yang W 1989 *Density Functional Theory of Atoms and Molecules* (New York: Oxford University Press)
[54] Koopmans T A 1934 *Physica* **1** 104